J Fluoresc (2014) 24:45–55
DOI 10.1007/s10895-013-1267-x

ORIGINAL PAPER

New Insights on the 7-azaindole Photophysics: The Overlooked Role of Its Non Phototautomerizable Hydrogen Bonded Complexes

Carmen Carmona · Emilio García-Fernández · José Hidalgo · Antonio Sánchez-Coronilla · Manuel Balón

Received: 8 May 2013 / Accepted: 8 July 2013 / Published online: 20 July 2013

Abstract In this paper we explore the formation and the photophysical properties of the scarcely studied open hydrogen bonded aggregates of 7-Azaindole, 7AI. Thus, we have analyzed the influence that the increase of the 7AI concentration and the decrease of the temperature have on the 7AI photophysics. To help the interpretation of the results, the 7AI-Pyridine system has been used as the model for the analysis of the photophysical properties attributable to the open $N_{pyrrolic} - H \cdots N_{pyridinic}$ hydrogen bonded aggregates. Also, the hydrogen bond interactions have been studied by means of the atom in molecule approach from the Bader theory. Experimental and theoretical results support that the formation of open hydrogen bonded aggregates, $(-7AI-)_n$ with $n \geq 2$ can efficiently compete with that of the profusely studied centrosymmetric cyclic dimer $(7AI)_2$. Moreover, these aggregates suffer a proton-driven electron transfer process that strongly quenches their room temperature fluorescence and, therefore, masks their presence in the 7AI solutions. Therefore, because most of the studies on the 7AI photophysics have been interpreted without considering the existence of such aggregates and, more important, ignoring its quenching process, many conclusions obtained from these studies should be carefully revised.

C. Carmona · J. Hidalgo · M. Balón (✉)
Departamento de Química Física, Facultad de Farmacia
Universidad de Sevilla, 41012 Sevilla, Spain
e-mail: balon@us.es

E. García-Fernández
Centro de Química Estructural, Instituto Superior Técnico,
Universidade Técnica de Lisboa, Complexo Interdisciplinar, Avd.
Revisco Pais 1, 1049-001 Lisbon, Portugal

A. Sánchez-Coronilla
Departamento de Química Física, Facultad de Ciencias,
Universidad de Cádiz, 11510 Puerto Real, Cádiz, Spain

Keywords 7-Azaindole · Hydrogen bonded aggregates · Proton-driven electron transfer

Introduction

More than 40 years ago, Kasha et al. [1] attributed the anomalous long Stokes shifted emission at 480 nm of 7-azaindole, 7AI, to the phototautomer of its cyclic c_{2h} dimer, $(7AI)_2$, Fig. 1. Since then, this photoreaction has been profusely studied [2] because it has been considered the paradigm of the light induced mutagenesis processes and the prototype of other molecular systems undergoing excited state double proton transfers. Noteworthy, despite it has been hypothesized on the presence, in the 7AI solutions, of hydrogen bonded complexes distinct from $(7AI)_2$, such as tetramers and chained oligomers [3–8], their implications in the 7AI photophysics have received much less attention. Thus, on one hand, it has been supposed that the oligomer population is very small and, on the other hand, because these aggregates are supposedly unable to experience the phototautomerization reaction, they have been considered as non-reactive species.

However, we have recently demonstrated that a compound structurally related to 7AI, 1-azacarbazole or α-carboline, AC, Fig. 1, forms highly reactive singly hydrogen bonded open dimers and higher aggregates [9]. These complexes experience an intermolecular photoinduced proton-driven electron transfer process that strongly quenches the fluorescence of the AC solutions at room temperature. Due to the close structural relationship between 7AI and AC, it can be presumed that similar reactive species could also be formed in the 7AI solutions. To verify this hypothesis, that could have important implications in the 7AI photophysics, we have studied the influence of the 7AI concentration and the temperature in the

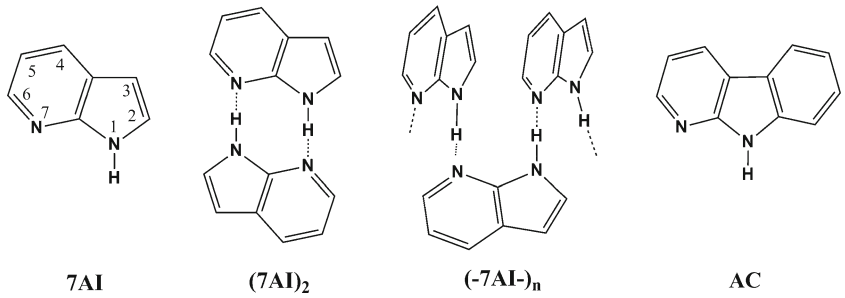

Fig. 1 Chemical structures of 7AI, $(7AI)_2$, $(-7AI-)_n$, and AC

7AI photophysics in low polar aprotic solvents. As for AC, to analyze the photophysics of the $N_{pyrrolic} - H\cdots N_{pyridinic}$ open hydrogen bonded aggregates the spectral properties of the 7AI-pyridine (Py) system have also been studied. Finally, the nature of the hydrogen bonded complexes has been theoretically analyzed by applying the atom in molecule, AIM, approach from the Bader theory [10].

Experimental

7AI, 4Azaindole, 4AI, and Py (≥97%) from Sigma-Aldrich, hexane and 2-methylbutane stored on molecular sieves, were used as purchased. Absorption and emission spectra were measured with a UV/Vis spectrometer Cary-100 and a fluorimeter Hitachi 2500. For the calculations of the absorption second derivative spectra, the Savitzky-Golay technique implemented in the Cary-100 computer was used [11]. Sample temperatures, ranged from 298 to 118 K were controlled by means of an Oxford DN1704 cryostat, purged with dried nitrogen, 99.99 % pure, equipped with an ITC4 controller interfaced to the spectrophotometers. It was found that, under these experimental conditions, the spectral changes induced by lowering the temperature were reversible. Time resolved fluorescence studies were investigated by using the time-correlated single-photon counting (SPC) technique in a FL-900CD Edinburgh Analytical Instrument. The excitation source, a nanosecond, nF900, flash lamp filled with 0.4 bar H_2, operated at 40 kHz with 7.5 kV applied across 1 mm electrode gap. Fluorescence kinetic constants were extracted by fitting profiles to computer-simulated exponential curves convoluted with instrument response functions.

Full optimization of the geometries has been performed by using density functional theory (DFT) bases approaches, in the context of the Becke's three-parameter hybrid functional with gradient correction provided by the Lee-Yang-Parr functional (B3LYP) [12, 13]. The cc-pVTZ basis sets on C and H and aug-cc-pVDZ basis set on N have been employed. The equilibrium structures have been characterized as real minima by the calculations of their second derivatives. The interaction energies for the complexes have been calculated after applying the zero-point energy correction (ZPE). The quantum mechanical computations have been carried out using the Gaussian 03 system [14]. Wavefunction analysis has been focused on the properties of the hydrogen bond adducts by employing the atoms in molecule approach of Bader, AIM [10], as implemented in the AIM2000 program [15]. The electron density and the Laplacian at the bond critical points, the ring critical points and some integrated properties have been calculated.

Results and Discussion

As previously observed for AC [9] and betacarboline (9H-pyrido[3,4-b]indole), BC [16], the addition of Py to a solution of 7AI in hexane broadens and shifts to the red the lowest energy absorption band of 7AI, spectra not shown. These spectral changes indicate that 7AI molecules associate with Py molecules by $N_{pyrrolic} - H\cdots N_{pyridinic}$ hydrogen bonds to produce complexes in the non polar solvent. The mean value of the ground state association constant for the formation of these 1:1 7AI-Py complexes, calculated as in previous works, is $8.8\pm0.6\ M^{-1}$. This value is similar to the value of $12.5\pm0.2\ M^{-1}$ and $20\pm2\ M^{-1}$ previously obtained for the formation constant of the AC-Py [9] and BC-Py [16] complexes in hexane, respectively.

The emission of the 7AI monomers in hexane, at 320 nm, is strongly quenched by the addition of Py, see Fig. 2. Interestingly, neither the shape nor the position of this UV band apparently changes with the increase of Py concentration. Thus, the $N_{pyrrolic} - H\cdots N_{pyridinic}$ hydrogen bonded complexes between 7AI and Py must be weakly fluorescent species at room temperature, see below. The Stern-Volmer plot of the relative fluorescence quantum yields of the 7AI-Py solutions, calculated as the ratio of the areas under the emission spectra, deviates upward, inset of Fig. 2. This indicates the simultaneous presence of a static and a dynamic quenching mechanism of the 7AI monomer. The dynamic component of the quenching has been evaluated by the Stern-Volmer plot of the mono-exponential fluorescence decay times of 7AI measured at the blue edge of the band and at different Py concentrations, inset of Fig. 2. The value of the

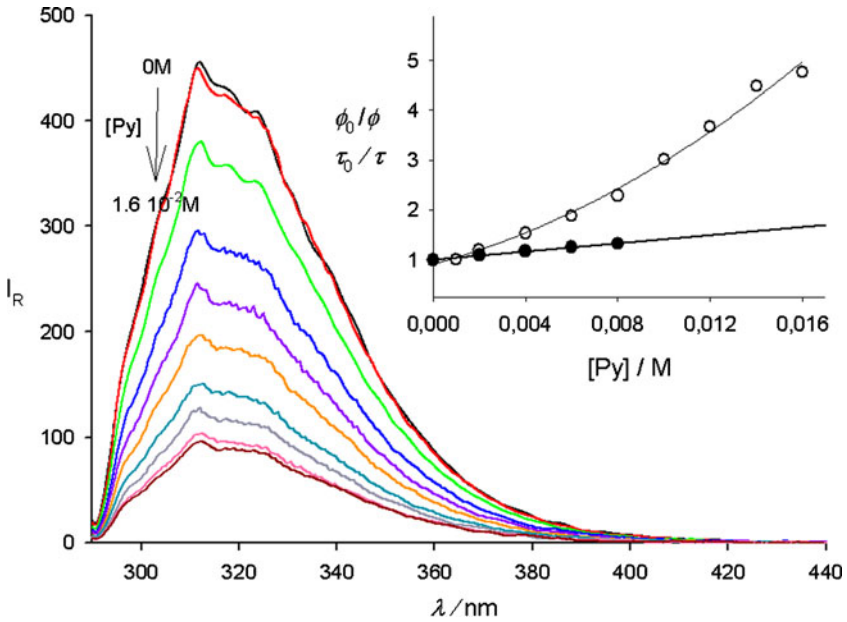

Fig. 2 Influence of Py addition on the room temperature emission spectrum of a 7AI solution 5 10^{-6} M in hexane, λ_{exc}=285 nm. In the inset, the Stern-Volmer plots of the relative quantum yields, taken as the areas under the emission spectra, ϕ_o/ϕ (*empty circle*), and the fluorescence decay times, τ_0/τ (*filled circle*), against the Py concentration

quenching rate constant, (2.7±0.3) 10^{10} M^{-1} s^{-1}, at 298 K, has the magnitude order typical of a diffusion-controlled reaction and it is similar to the value (2.3±0.3) 10^{10} M^{-1} s^{-1} previously reported for the AC-Py system at the same temperature.

These experimental observations can be rationalised by using a mechanism similar to that previously proposed for the AC-Py system, Fig. 3 [9]. According to this mechanism, the 7AI monomer interacts with Py in both the ground and the excited states. The $N_{pyrrolic} - H\cdots N_{pyridinic}$ 7AI-Py hydrogen bonded complexes experience, in the excited state, a quenching process, k_2, similar to that reported for other intermolecular hydrogen bonded aromatic chromophores [9, 16–20]. Mataga et al. [21], proposed that this highly efficient deactivation of fluorescence states can be explained in terms of curve-crossing dynamics involving a biradicaloid dark charge transfer state. The model of these authors, confirmed by computational studies carried out by Sobolewski et al. [22, 23], assumes that the proton movement along the hydrogen bond, in the excited state, induces an electron transfer that quenches the fluorescence [21].

To get further insights on this fluorescence quenching process, the influence of the temperature decrease in the emission spectra of the 7AI-Py hydrogen bonded complexes has been analyzed. These variable temperature experiments have been carried out using 2-methylbutane as the solvent. This solvent, with similar polarity than hexane, allows studying the liquid solutions in a wider temperature range because its significantly lower melting point. The influence of the temperature on the fluorescence spectra has been measured for a solution 5 10^{-6} M of 7AI and 1 M of Py, Fig. 4. These concentrations have been selected to minimize the possible 7AI self dimerization upon the temperature decrease. Thus, under these conditions, the proportion of the 7AI-Py hydrogen bonded complex can be estimated greater than 90 % and, therefore, in the fluorescence spectra at room temperature only a tiny emission from the monomer, at 320 nm, is observed. As can be seen in Fig. 4, the influence of the temperature decrease on the emission spectra of this solution reveals an interesting feature of this quenching process: The appearance of a new red shifted emission band, at 350 nm, that progressively grows up upon decreasing the temperature. Again, this behaviour is completely

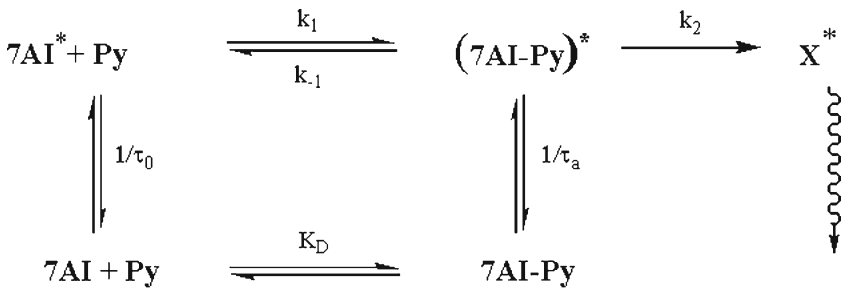

Fig. 3 Ground and excited state hydrogen bonding interaction mechanisms between 7AI and Py

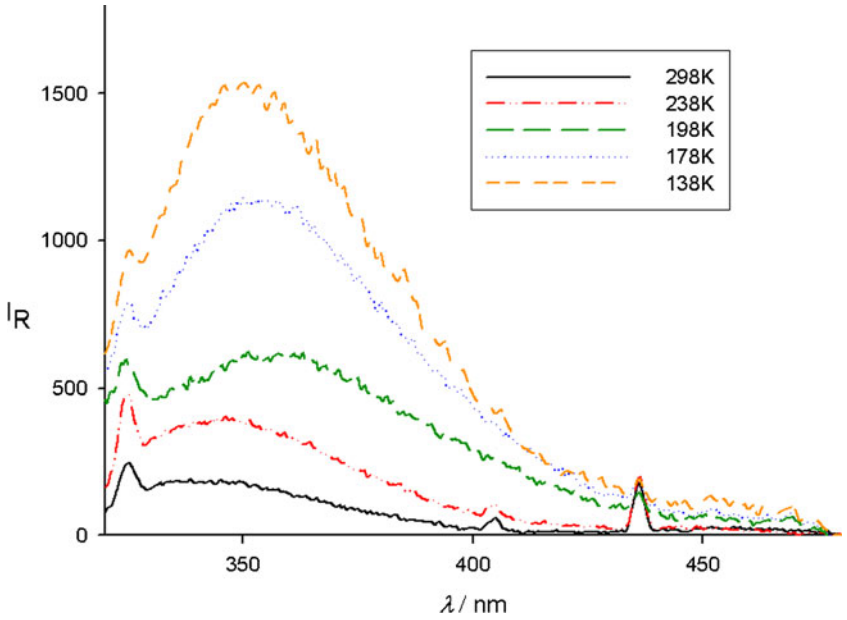

Fig. 4 Influence of the temperature on the emission spectra, λ_{exc}=295 nm, of a 7AI 5 10^{-6} M plus Py 1 M solution in 2 MB

similar to that previously reported for AC-Py and BC-Py systems. Thus, this new emission must be ascribed to the $N_{pyrrolic} - H\cdots N_{pyridinic}$ hydrogen bonded 7AI-Py complexes. According to the mechanism in Fig. 3, the enhancement of the emission intensity of these hydrogen bonded complexes at low temperatures can be related with the expected progressive decrease of k_2 with the temperature decrease. As the temperature decreases k_2 diminishes becoming similar or smaller than the radiative rate constant of the 7AI-Py complexes. Therefore, at the lowest temperatures, the quenching becomes inoperative and the emission intensity of the $N_{pyrrolic} - H\cdots N_{pyridinic}$ complexes maximizes.

Figure 5 shows that the lowest absorption band of 7AI in hexane broadens and grows at 310 nm with an increase in the 7AI concentration. Although these changes have been usually interpreted as due to the direct transformation of the 7AI monomer into the $(7AI)_2$ dimer, neither isosbestic nor isoclinic points, inset of Fig. 5, are observed in the absorption and second derivative spectra, respectively. Moreover, the value of the dimerization constant, determined as elsewhere [24, 25], decreases as the monitored absorption wavelength increases reaching values around 2 10^3 M^{-1} similar to those reported by other authors [24, 25]. This behaviour, hardly attributable to the sole formation of $(7AI)_2$, could be

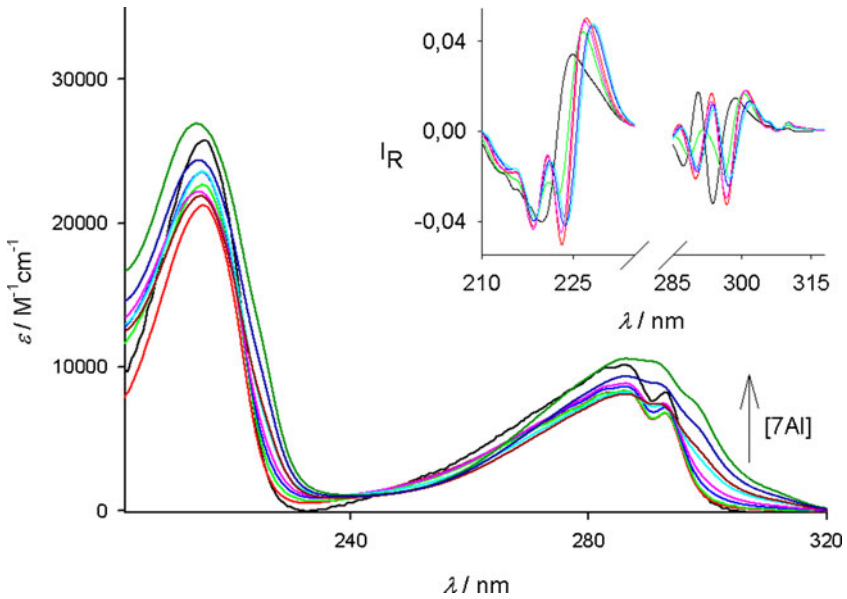

Fig. 5 Concentration normalized room temperature absorption spectra of solutions with increasing concentrations of 7AI, 10^{-6}–10^{-2} M, in hexane. In the inset, the absorption second derivative spectra

reasonably explained assuming the additional formation of other 7AI hydrogen bonded species.

As previously observed [24–28], the emission spectra of the 7AI solutions, at different 7AI concentrations, markedly depend on the 7AI concentration, the excitation wavelength and the temperature. Figure 6a typically shows that at $\lambda_{exc} \leq 300$ nm, the 7AI monomer emission at 320 nm is the only band of the 7AI dilute solutions. Upon increasing the 7AI concentration, the intensity of this band diminishes and, at 7AI concentrations above 10^{-4} M, the weak emission band of the $(7AI)_2$ phototautomer, at 480 nm, becomes perceptible. Noteworthy, contrary to that generally assumed, the quenching of the 320 nm emission band is not only due to the static ground state dimerization of the 7AI monomers, but a dynamic component also operates. Thus, as previously reported by Takeuchi and Tahara [26], the monoexponential decay times, measured at the blue edge of this band, significantly diminish upon increasing the 7AI concentration. The dynamic quenching constant estimated from the Stern-Volmer plot in the inset of Fig. 6a, $(3\pm0.5)\ 10^{10}\ M^{-1}\ s^{-1}$, is entirely

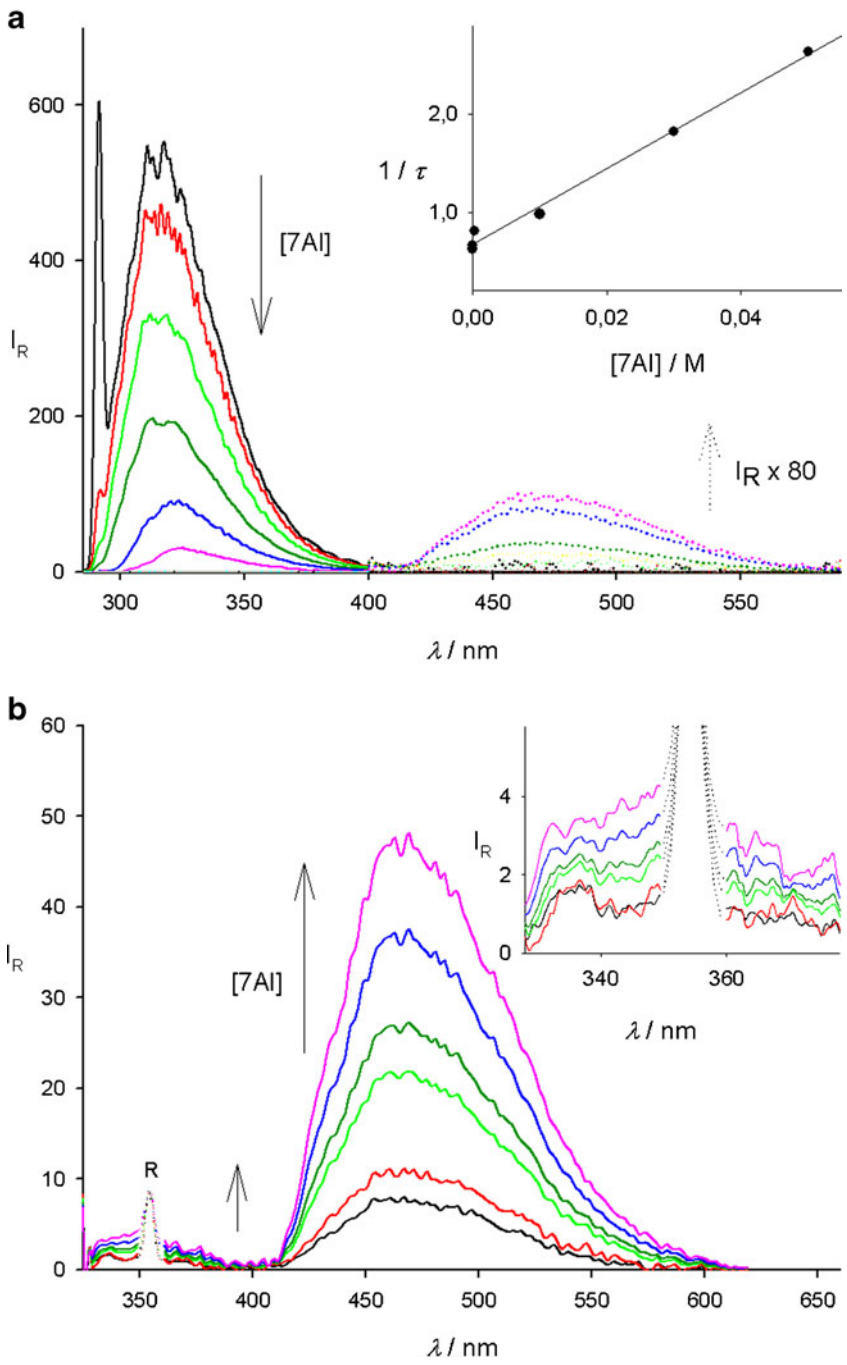

Fig. 6 Room temperature emission spectra of solutions with increasing concentrations of 7AI, 10^{-6}–10^{-2} M, in hexane at: **a** λ_{exc}=290 nm and **b** λ_{exc}=315 nm. In the insets: (6a) 1/τ (*filled circle*) against the 7AI concentration and (6b) Emission spectra in the 300–400 nm wavelength range at λ_{exc}=315 nm. R denotes Raman band

similar to that calculated in this work for the 7AI-Py system and those reported for other related systems [18–20].

Figure 6b shows that, for a given 7AI concentration, the emission band at 480 nm becomes more prominent as the excitation wavelength increases and the monomer absorption progressively diminishes. Also, a tiny emission, red shifted with respect to the monomer emission, at 350 nm, is observed, see inset of Fig. 6b. This ultraviolet emission, also distinguishable at low 7AI concentrations, cannot be due to the monomer emission because it is present at $\lambda_{exc} \geq 305$ nm where the monomer does not absorb. Neither it can be ascribed to the emission from the $(7AI)_2$ dimer. Thus, Takeuchi and Tahara [28], also observed this band, at 350 nm, in a room temperature concentrated 7AI solution at $\lambda_{exc}=313$ nm. According to the authors, this emission could not be due to the $(7AI)_2$ complex because the double proton transfer process in this complex is highly efficient at room temperature and, therefore, the $(7AI)_2$ fluorescence can be only noticeable in the femtosecond time resolved measurements. The authors then supposed that this band should be due to a small population of aggregate species different from $(7AI)_2$. This, together with the fact that this emission reminds the fluorescence band showed in Fig. 4 and ascribed to non cyclic $N_{pyrrolic} - H\cdots N_{pyridinic}$ hydrogen bonded complexes formed in the 7AI-Py system, let us to assume that species such as those shown in Fig. 1, can be responsible for this red shifted emission.

If this is so, the studies of the temperature influence could help to confirm this hypothesis. For these studies a highly dilute solution of 7AI has been selected in order to assure the exclusive presence of the 7AI monomer at room temperature.

As Fig. 7a shows, at $\lambda_{exc}=290$ nm the intensity of the emission band of the 7AI monomer progressively decreases and below 198 K another red shifted structured fluorescence band centred at 350 nm begins to appear, Fig. 7a. This new band is practically the only emission observed at $\lambda_{exc} \geq 305$ nm, Fig. 7b. Catalán has recently attributed this emission to certain $(7AI)_2$ "trapped dimers" that, because of the low temperatures, have not enough energy to surmount the barrier for the tautomerization process [29]. However, as before mentioned, this band is observed at room temperature, Fig. 6b, and at different 7AI concentrations. Furthermore, the changes observed in the 7AI emission spectrum, upon lowering the temperature, are completely similar to those get for 7AI-Py and other related systems such as AC-Py, BC-Py, AC, BC and 4AI, that do not form cyclic dimers [9, 17]. In fact, this band excellently matches those of 7AI-Py and $(-4AI-)_2$ complexes at 138 K, inset of Fig. 7a, and it is equal to that reported for the 7AI tetramer in the solid [30]. Therefore, the emission band at 350 nm, clearly observed at low temperatures, Fig. 7, is due, as that observed in the room temperature steady state spectrum, inset of Fig. 6b, to the presence of 7AI non phototautomerizable hydrogen bonded aggregates, see Fig. 1.

Accordingly, if we assume for these 7AI complexes the photophysical mechanism in Fig. 3, the intensity increase of the band at 350 nm, upon decreasing the temperature, should be, as in the 7AI-Py system, related with the decrease of k_2 with the lowering of the temperature. Thus, at sufficiently low temperatures, once the 7AI complexes are formed and under photo stationary conditions, the following modified Stern-Volmer equation can be derived [9, 17],

$$\frac{\varphi^0}{\varphi} = 1 + k_2\,\tau^0 = 1 + \frac{k_2}{k_r} \tag{1}$$

Where φ^0 and φ represent the fluorescence quantum yields, i.e. the areas under the emission spectra of the unquenched and quenched complexes and k_r and τ^0 ($k_r=1/\tau^0$) their radiative rate constants and the fluorescence lifetimes, respectively. Since k_r should not change with the temperature, the relative quantum yield, φ^0/φ, would decrease as k_2 diminishes and, at sufficiently low temperatures, the quenching process completely disappears and $\varphi \approx \varphi^0$. By using the Arrhenius relation, the Eq. 2 can be derived:

$$\ln k_2 = \ln\left(\varphi^0/\varphi - 1\right) = -E_A/RT + cte \tag{2}$$

From the plot in the inset of Fig. 7b a value of 1.7 kcal-mol^{-1} can be estimated for the activation energy of the photoinduced proton driven electron transfer process experienced by these 7AI aggregates. This value is similar to those of 1.4 kcal mol^{-1} and 1.0 kcal mol^{-1} reported for a similar process suffered by the non cyclic hydrogen bonded complexes of AC and BC, respectively [9, 17]. Noteworthy, these values are also remarkably close to that of 1.4 kcal-mol^{-1} previously reported for the 7AI system but ascribed to the intrinsic energy barrier of the photoinduced double proton transfer experienced by the $(7AI)_2$ dimer [24, 29, 31].

The formation of the 7AI aggregates different from the cyclic $(7AI)_2$ complex is, on the other hand, very plausible from a mechanistic point of view. Thus, it is reasonable to suppose that the initial hydrogen bond interaction between the pyridinic nitrogen and the pyrrolic proton would give rise to the formation of a singly hydrogen bonded dimer, $(-7AI-)_2$. Later on, this dimer could cyclise to produce $(7AI)_2$ or, alternatively, it could continue the aggregation process adding new 7AI molecules to form $(-7AI-)_n$ complexes as those shown in Fig. 1. Moreover, those open aggregates with the adequate structure can form cyclic oligomers as the basket-like tetramers, $(7AI)_4$, constituting the structural unit of the 7AI crystal [32]. These tetramers have been proposed by Fedor and Korter [7] to explain the terahertz time domain experimental spectra of the 7AI solutions at room temperature. It must be noted that the formation of the $(7AI)_4$ necessary implies the existence of their open chain trimer and tetramer precursors. Nevertheless, because the commonly accepted great stability of $(7AI)_2$, as compared with other dimeric structures, the population of hydrogen bonded complexes distinct from the cyclic dimer has

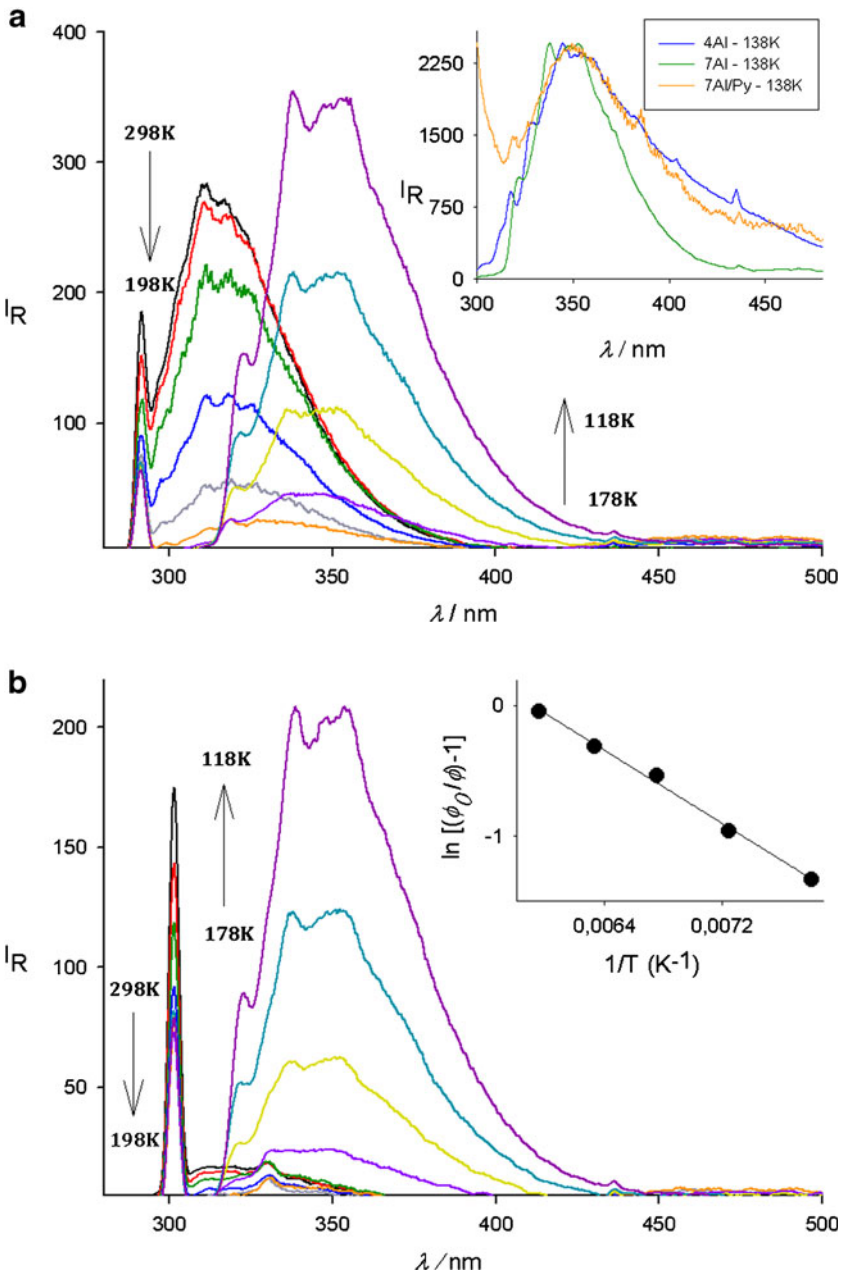

Fig. 7 Temperature influence on the emission spectra of a 7AI solution, 5 10^{-6} M, in 2-methyl butane, 2 MB, obtained at **a** λ_{exc}=290 nm and **b** λ_{exc}=305 nm. In the insets: (7a) the normalized emission spectra of a 7AI 5 10^{-6} M plus Py 1 M, a 4AI solution, 5 10^{-6} M, and a 7AI solution, 5 10^{-6} M, in 2 MB at 138 K, λ_{exc}=290 nm and (7b) Arrhenius plot according to Eq. 2

been usually considered negligible. This could be possibly the reason why the systematic study on the relative stability of the dimers and higher order aggregates has never been carried out.

As in a previous work [33], to theoretically analyze the hydrogen bond interactions of 7AI, the atom in molecule approach, AIM, from the Bader theory [10] has been applied. This theory has demonstrated to be very useful in the analysis of different intermolecular interactions and, in particular, the hydrogen bond interactions. In fact, it has fully supported the hypothesis, postulated from our experimental studies, on the nature and properties of the hydrogen bond complexes formed between a related heteroaromatic ring, BC, and different hydrogen bond donors [33]. Thus, the properties of the bond critical point as the electron density at the bond critical point, ρ, and its Laplacian, $\nabla^2\rho$, reveal the characteristics of the interactions. Therefore, apart from the well known $(7AI)_2$ dimer, we have applied the AIM theory to the singly hydrogen bonded 7AI-Py, $(-7AI-)_2$ and $(-AC-)_2$ dimers, the open $(-7AI-)_3$ trimer and the $(7AI)_4$ tetramer. As typically shown in Fig. 8, the first topological criterion of the existence of a hydrogen bond is fulfilled: bond critical points indeed appear where they are expected, i.e. between the pyridinic and pyrrolic nitrogen atoms of the partners. Moreover, the concomitant bond path links these two atoms. The selected AIM parameters, the electron density and its Laplacian at the bond critical point along the $N_{pyrrolic} - H\cdots N_{pyridinic}$ bond paths, together with the formation enthalpies for the different complexes are reported in

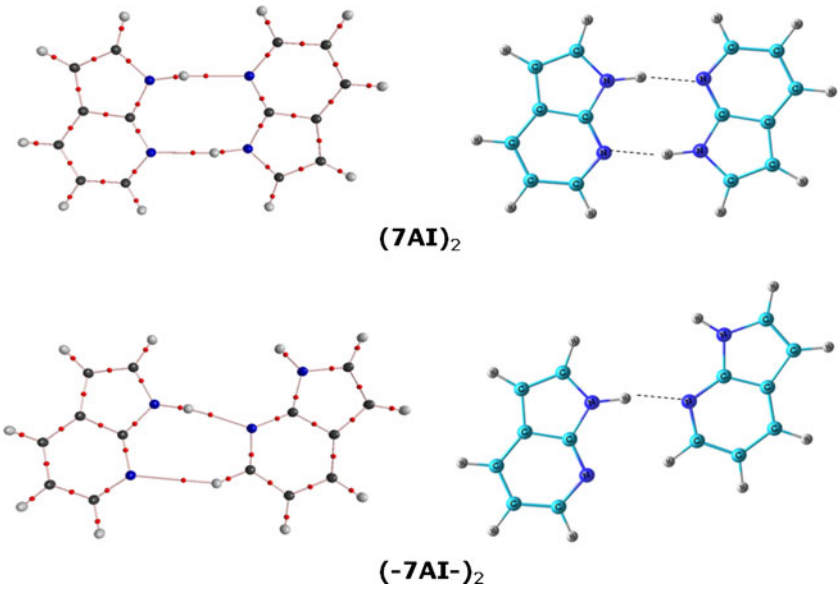

Fig. 8 Molecular graphs of $(7AI)_2$ and $(-7AI-)_2$ complexes. The small red circles and lines in the left side graphs represent the bond critical points and bond paths, respectively

Table 1. As can be seen in this Table, there is an excellent concordance between the enthalpies obtained in the present work and those reported for the $(7AI)_2$ dimer and tetramer formation. It should be also mentioned that in the $(-7AI-)_2$, in the $(-AC-)_2$ and in the $(-7AI-)_3$ complexes a bond critical point also appears between the free pyridinic nitrogen of one molecule and the CH group adjacent to the pyridinic nitrogen, of the other molecule, involved in the $N_{pyrrolic} - H\cdots N_{pyridinic}$ bond, Fig. 8. However, the corresponding ρ and $\nabla^2\rho$ values are very low indicating an extremely weak $N_{pyridinic}\cdots H - C$ bond and, therefore, they have not been included in the Table.

The data in Table 1 show that all the studied hydrogen bond interactions are weak or close-shell interactions. Thus, while the $N_{pyrrolic} - H$ bond keeps the characteristics of a covalent bond, the magnitudes and sign of the AIM parameters indicate that the $N_{pyridinic}\cdots H$ is a weak hydrogen bond interaction. As expected, the $N_{pyrrolic} - H\cdots N_{pyridinic}$ bonds in $(-AC-)_2$ have the same characteristics than those in $(-7AI-)_2$ and both dimers have also equal formation enthalpies. Interestingly, the formation enthalpies depend linearly upon the number of hydrogen bonds, Fig. 9. This fact, previously observed by Fedor and Korter [7], indicates that, contrary to that generally assumed, there is not an extra stabilization in the formation of the $(7AI)_2$ complex but the formation enthalpy merely reflect the presence of two hydrogen bonds in the complex. Thus, in all the complexes analyzed, the nature of the hydrogen bonds is completely similar and the stabilization energies per hydrogen bond are, as Fig. 9 shows, the same. Therefore, from an energetic point of view once the open $(-7AI-)_2$ hydrogen bonded complex is formed, it can indistinctly cyclise or continue the aggregation process adding a new 7AI molecule to produce $(-7AI-)_3$, and higher order aggregates, see Table 1. In this sense, the high value obtained for the experimental dimerization constant of 7AI [24, 25], is not due, as previously proposed [24], to a cooperative effect resulting from the resonance interaction between the 7AI rings in the $(7AI)_2$

Table 1 Electron density, ρ, and its Laplacian, $\nabla^2\rho$, in arbitrary units, at the bond critical points along the $N_{pyrrolic} - H\cdots N_{pyridinic}$ bond paths and the formation enthalpies, ΔH, in kcal mol^{-1}, for the hydrogen bonded complexes

System	$N_{pyrrolic} - H$		$H\cdots N_{pyridinic}$		*-ΔH*
	ρ	$\nabla^2\rho$	*ρ*	$\nabla^2\rho$	
7AI-Py	*0.333*	*−1.972*	*0.010*	*0.030*	*6.3*
$(7AI)_2$	*0.329*	*−1.963*	*0.032*	*0.069*	*12.5(12.7)*[a]
$(-7AI-)_2$	*0.334*	*−1.981*	*0.028*	*0.068*	*5.2*
$(-AC-)_2$	*0.334*	*−1.970*	*0.028*	*0.068*	*4.8*
$(-7AI-)_3$	*0.332*	*−1.974*	*0.030*	*0.070*	*13.3*
	0.338	*−1.977*	*0.029*	*0.069*	
$(7AI)_4$	*0.328*	*−1.960*	*0.034*	*0.071*	*26.4(26.6)*[a]
	0.328	*−1.960*	*0.034*	*0.071*	
	0.328	*−1.961*	*0.034*	*0.071*	
	0.328	*−1.961*	*0.034*	*0.071*	

[a] Taken from Reference 7

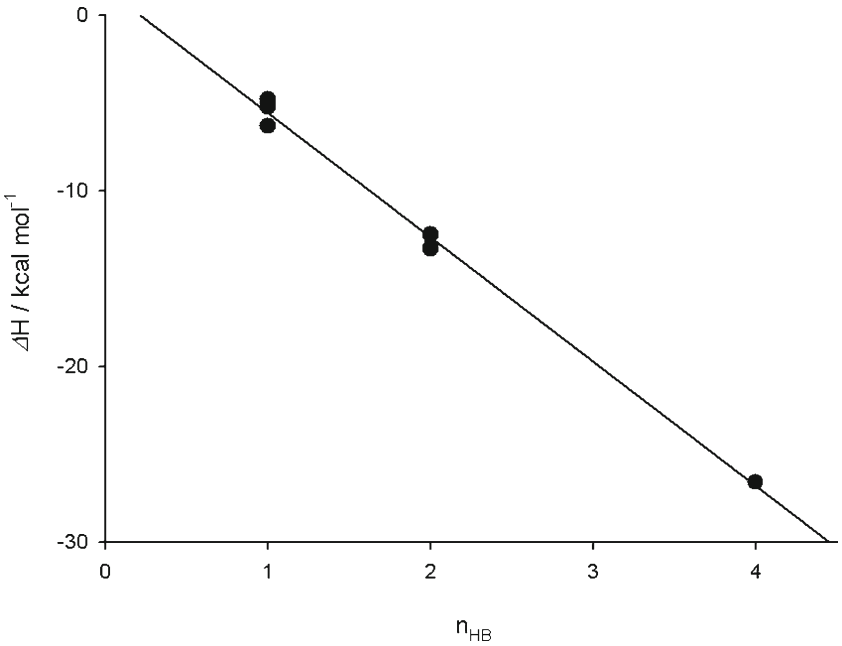

Fig. 9 Relationship between the formation enthalpies and the number of hydrogen bonds in the complexes (n_{HB})

complex. Conversely, this apparent association constant embodies the different self-association steps occurring in the 7AI solutions. Moreover, the simultaneous presence of different hydrogen bonded complexes help to understand the aforementioned absence of the isosbestic and isoclinic points in the absorption and second derivative spectra, respectively.

These data also indicate that, since the successive hydrogen bond interactions in the 7AI complexes are similar, the spectroscopic characteristics of the different hydrogen bonded complexes should be similar too. Also, due to the larger enthalpies for the higher order aggregate formation, these species should be efficiently stabilized at the lowest temperatures. Therefore, although the emission, at 350 nm, observed in the 7AI solutions at the lowest temperatures could be ascribed, as reported by Catalán, to a trapped $(7AI)_2$ complex that cannot suffer the double proton transfer, we better believe that, as for 7AI-Py, AC and BC, this emission in the 7AI solutions is mainly due to the unquenched non phototautomerizable $(-7AI-)_n$ hydrogen bonded aggregates. The fact that the activation energy for the proton driven electron transfer quenching process is the same for the complexes of 7AI, AC and BC further supports this statement. Finally, the quenching process suffered by the 7AI aggregates nicely explains the origin of the tiny emission, at 350 nm, observed, at room temperature, in this paper and by Takeuchi and Tahara in the concentrated solutions of 7AI. As mentioned, the authors ascribed this emission to the small population of 7AI oligomers. Thus, we agree with the emitting species being different from the $(7AI)_2$ complex but the low intensity of this band is not caused, as the authors proposed, by the small population of the 7AI aggregates but it is due to the high efficiency, at room temperature, of the proton driven electron transfer quenching process experimented by these species.

Summary and Conclusions

Although it is commonly accepted that the photophysics of 7AI in low polar aprotic solvents is almost exclusively determined by the formation of its readily phototautomerizable cyclic dimers $(7AI)_2$, this paper highlights some experimental results that could hardly be explained on this basis. These results can be briefly summarized as follows: i) The absence of isosbestic and isoclinic points in the absorption and second derivative absorption spectra of the 7AI solutions with increasing the 7AI concentration and the different values of the dimerization constant calculated from the absorbance titration data obtained at different wavelengths, ii) The dynamic quenching of the emission band of the 7AI monomer at 320 nm upon increasing the 7AI concentration and the appearance of a weak emission band at 350 nm together with the strong enhancement of this band intensity upon decreasing the temperature.

The theoretical calculations carried out in this work and the similarity among these results and those observed for other related systems, that cannot form cyclic hydrogen bonded dimers, led us to attribute these experimental findings to the formation of non phototautomerizable $(-7AI-)_n$ aggregates. Accordingly, the simultaneous ground state formation of $(7AI)_2$ and $(-7AI-)_n$ species could nicely explain the aforementioned absence of isosbestic and isoclinic points in the absorption spectra and the wavelength dependent values of the apparent dimerization constant of 7AI. Furthermore, the excited state formation of these kinds of $(-7AI-)_n$ aggregates could also justify the quenching of the 7AI monomer emission and the appearance of the emission band at 350 nm. By analogy with the model 7AI-Py and other related systems, the band at 350 nm is, at room temperature, extremely weak because of the photoinduced proton driven electron transfer process occurring in the $(-7AI-)_n$ aggregates

strongly quenches their emission. This quenching is probably the reason why the role played by the $(-7AI-)_n$ aggregates in the photophysics of 7AI has been systematically overlooked in previous studies. Nevertheless, as the temperature decreases and, consequently, the efficiency of the quenching process diminishes, the emission of the $(-7AI-)_n$ aggregates becomes more evident in the fluorescence spectrum of 7AI. Therefore, because most of the studies on the 7AI photophysics have overlooked the role played by these non phototautomerizable 7AI aggregates, we can conclude that many aspects on our current knowledge of the 7AI photophysics should be carefully revised.

Acknowledgment We gratefully acknowledge financial support from the Junta de Andalucía, FQM-106. Calculations were done through CICA, Centro Informático Científico de Andalucía, Spain.

References

1. Taylor C, El-Bayoumi A, Kasha M (1969) Excited-state two-proton tautomerism in hydrogen-bonded N-Heterocyclic base pairs. Proc Natl Acad Sci USA 63:253–260
2. For a recent review see: Sekiya H, Sakota K (2008) Excited-state double-proton transfer in a model DNA base pair: resolution for stepwise and concerted mechanism controversy in the 7-Azaindole dimer revealed by Frequency and time-resolved spectroscopy. Photochem Photobiol C: Photochem Rev 9: 81–91
3. Bulska H, Grabowski A, Pakula B, Sepiol J, Waluk J, Wild UP (1984) Spectroscopy of doubly hydrogen-bonded 7-Azaindole. Reinvestigation of the excited state reaction. J Luminescence 29:65–81
4. Fuke K, Kaya K (1989) Dynamics of double-proton-transfer reaction in the excited-state model hydrogen-bonded base pairs. J Phys Chem 93:614–621
5. Catalán J (2002) On the evidence obtained by exciting 7-Azaindole at 320 nm in 10–2 M solutions. J Phys Chem 106:6738–6742
6. Walmsly J (1981) Self-association of 7-Azaindole in Nonpolar Solvents. J Phys Chem 85:3181–3187
7. Fedor AM, Korter TK (2006) Terahertz spectroscopy of 7-Azaindole clusters in solution. Chem Phys Lett 429:405–409
8. Lim H, Park S, Jang D (2011) Excited-state double proton transfer of 7-Azaindole dimers in a low-temperature organic glass. Photochem Photobiol 87:766–771
9. García-Fernández E, Carmona C, Muñoz MA, Hidalgo J, Balón M (2012) A photophysical study of the α-Carboline (1-Azacarbazole) aggregation process. Photochem Photobiol 88:277–284
10. Bader RFW (1994) Atoms in molecules. A quantum theory. Clarendon, Oxford, 1994
11. Savitzky A, Golay MJE (1964) Smoothing and differentiation of data by simplified least squares procedures. Anal Chem 36:1627–1639
12. Becke ADJ (1993) A new mixing of Hartree-Fock and local density-functional theories. J Chem Phys 98:5648–5652
13. Lee C, Yang W, Parr RG (1988) Development of the Colle-Salvetti correlation-energy formula into a functional of the electron density. Phys Rev B 37:785–789
14. Frisch MJ, Trucks GW, Schlegel HB, Scuseria GE, Robb MA, Cheeseman JR, Montgomery JAJ, Vreven T, Kudin KN, Burant JC, Millam JM, Iyengar SS, Tomasi J, Barone V, Mennucci B, Cossi M, Scalmani G, Rega N, Petersson GA, Nakatsuji H, Hada M, Ehara M, Toyota K, Fukuda R, Hasegawa J, Ishida M, Nakajima T, Honda Y, Kitao O, Nakai H, Klene M, Li X, Knox JE, Hratchian HP, Cross JB, Bakken V, Adamo C, Jaramillo J, Gomperts R, Stratmann RE, Yazyev O, Austin AJ, Cammi R, Pomelli C, Ochterski JW, Ayala PY, Morokuma K, Voth GA, Salvador P, Dannenberg JJ, Sakrzewski VG, Dapprich S, Daniels AD, Strain MC, Farkas O, Malick DK, Rabuck AD, Raghavachari K, Foresman JB, Ortiz JV, Cui Q, Baboul AG, Clifford S, Cioslowski J, Stefanov BB, Liu G, Liashenko A, Piskorz P, Komaromi I, Martin RL, Fox DJ, Keith T, Al-Laham MA, Peng CY, Nanayakkara A, Challacombe M, Gill PMW, Johnson B, Chen W, Wong MW, Gonzalez C, Pople JA (2003) Gaussian 03, revision D.0. Gaussian Inc, Pittsburgh
15. Biegler-König F, Schönbohm J (2002) Update of the AIM2000-Program for atoms in molecules. J Comp Chem 23:1489–1494
16. Hidalgo J, Sánchez-Coronilla A, Muñoz MA, Carmona C, Balón M (2007) Fluorescence Quenching of Betacarboline (9H-pyrido [3,4-b]indole) induced by intermolecular hydrogen bonding with pyridines. J Luminescence 127:671–677
17. Hidalgo J, Sánchez-Coronilla A, Balón M, Muñoz MA, Carmona C (2009) Dual emission of temperature-induced betacarboline self-associated hydrogen bond aggregates. Photochem Photobiol Sci 8:414–420
18. Martín M, Ikeda N, Okada T, Mataga N (1982) Picosecond laser photolysis studies of deactivation processes of excited hydrogen-bonding complexes. 2. Dibenzocarbazole-pyridine systems. J Phys Chem 86:4148–4156
19. Miyasaka H, Tabata A, Ojima S, Ikeda N, Mataga N (1993) Femtosecond-picosecond laser photolysis studies on the mechanisms of fluorescence quenching induced by Hydrogen-Bonding Interactions: 1-Pyrenol-pyridine systems. J Phys Chem 97:8222–8228
20. Herbich J, Kijak M, Zielinska A, Thummel RP, Waluk J (2002) Fluorescence quenching by pyridine and derivatives induced by intermolecular hydrogen bonding to pyrrole-containing heteroaromatics. J Phys Chem 106:2158–2163
21. Mataga N, Chosrowjan H, Taniguchi S (2005) Ultrafast charge transfer in excited electronic states and investigations into fundamental problems of exciplex chemistry: our early studies and recent developments. J Photochem Photobiol C: Photochem Rev 6:37–79
22. Sobolewski AL, Domcke W (2007) Computational studies of the photophysics of hydrogen-bonded molecular systems. J Phys Chem 111:11725–11735
23. Lan Z, Frutos L, Sobolewski A, Domcke W (2008) Photochemistry of hydrogen-bonded aromatic pairs: quantum dynamical calculations for the pyrrole–pyridine complex. Proc Natl Acad Sci USA 105:12707–12712
24. Ingham KC, El-Bayoumi MA (1974) Photoinduced double proton transfer in a model hydrogen bonded base pair. Effects of temperature and deuterium substitution. J Am Chem Soc 96:1674–1682
25. Kwon OH, Zewail AH (2007) Double proton transfer dynamics of model DNA base pairs in the condensed phase. Proc Natl Acad Sci USA 104:8703–8708
26. Takeuchi S, Tahara T (1998) Femtosecond ultraviolet–visible fluorescence study of the excited-state proton-transfer reaction of 7-Azaindole dimer. J Phys Chem A 102:7740–7753
27. Catalán J, Kasha M (2000) Photophysics of 7-Azaindole, Its Doubly-H-Bonded base-pair, and corresponding proton-transfer-tautomer dimeric species, via defining experimental and theoretical results. J Phys Chem A 104:10812–10820
28. Takeuchi S, Tahara T (2007) Femtosecond ultraviolet–visible fluorescence study of the excited-state proton-transfer reaction of 7-Azaindole dimer. Proc Natl Acad Sci USA 104:5285–5290
29. Catalán J (2010) Activation energy of the two-proton phototautomerism in 7-Azaindole dimer and its medium-dependence. J Phys Chem A 114:5666–5673
30. Chou P, Liao J, Wei C, Yang C, Yu W, Chou Y (2000) Excited-state double proton transfer on 3-Iodo-7-Azaindole dimer in a single crystal. J Am Chem Soc 122:986–987
31. Douhal A, Kim SK, Zewail AH (1995) Femtosecond molecular dynamics of tautomerization in model base pairs. Nature 3:260–263

32. Dufour P, Dartiguenave Y, Dartiguenave M, Dufour N, Lebuis AM, Bélanger-Gariépy F, Beauchamp AL (1990) Crystal structures of 7-Azaindole, an unusual hydrogen-bonded tetramer, and of two of its Methylmercury(II) complexes. Can J Chem 68:193–201

33. Sánchez-Coronilla A, Balón M, Sánchez-Marcos E, Muñoz MA, Carmona C (2010) A theoretical study of the hydrogen bond donor capability and co-operative effects in the hydrogen bond complexes of the Diaza-aromatic Betacarbolines. Phys Chem Chem Phys 12:5276–5284